Color of wood under various conditions of illumination

Alfred Rinnhofer*, Wanda Benesova**, Gerhard Jakob***, Roman Benes****

Joanneum Research
Institute of Digital Image Processing
Wastiangasse 6, A-8010 Graz, Austria

alfred.rinnhofer@joanneum.at,
wanda.benesova@joanneum.at
gerhard.jakob@joanneum.at

Abstract

To design a wood inspection system, including color as a relevant parameter, it is necessary to know about the particular relations between illumination and viewing conditions and the anisotropic characteristics of wood surfaces. Color is the perceptual result of light in the visible region of the spectrum and, hence, the evaluating criteria are derived from human observation. The goal of this work is to investigate the change of measured color of different wood species under varying illumination conditions. We demonstrate, that for different wood species the observed color changes in relation to the incidence angle of illumination. The change is related to the orientation of the grain according to the illumination direction. To compare the measured color deviation with technological limitations of color measurements performed with state of the art 3 x 8 Bit color linescan cameras, several simulations for such a type of camera are presented in addition.

1. Introduction

Today wood industry has a strong need for industrial inspection systems for wood grading to guaranty higher product quality and even better defined products with more different grades than ever before. Human graders, although they all are wood experts, can no longer fulfill these requirements because of speed and accuracy limitations. Therefore automatic inspection systems should take over this important task.

Several industrial inspection systems are already successfully installed in the wood industry. For softwood lumber inspection, multi- sensor systems are the state of the art. The cameras are responsible only for the detection of surface defects. For other type of defects like wane or sound knots additional sensor systems (e. g. “sheet of light” 3D measurement, X-ray, etc.) are added. So each subsystem can focus on those tasks for which it is best suited.

In parquet industry, due to the normally well-defined shape of parquet strips, a big demand (mainly to avoid additional costs) for systems with only one camera per side exists. These cameras should deliver images that contain all the necessary information to successfully perform a quality grading. The main tasks for parquet inspection are:

- High precision measurement of rectangular strips
- Object recognition: knots, cracks, edge defects, worm-holes
- Texture grading: all grain related appearance patterns
- Color grading: including sapwood detection, decay, brown heart, red, blue and yellow stain, color variations after steam and heat treatment, …

Objects like cracks and wormholes very often can only be discriminated from other wood regions like high contrast grain, pith rays or pin knots by making their 3D structure as visible as possible in the image. A flat illumination can highlight the 3D information by giving clear and strong shadows.

For the best discrimination of these types of surface defects, a flat illumination is a big advantage. When we were starting the development of a new, color based parquet-grading system a few years ago, we had the background knowledge of years of experience in image processing of black and white images of wood. Knowing the problems with these systems, we certainly wanted to set up illumination in a position to get maximum shadows for all kind of surface defects. By optimizing in this direction, and ignoring the (not really known) influence of the illumination / camera geometry for color grading, we lost the color information at a certain point nearly completely. Color grading, and even more color measurement require very different camera and illumination arrangements. This paper helps to find a good compromise between these two contrary needs.

Representation and measurement of color

Color is the perceptual result of light in the visible region of the spectrum, having wavelengths from 400 nm to 700 nm. The color stimuli are assumed to be uniquely defined by their radiant power spectral distributions. In the complete specification of each color stimulus, it is necessary to know not only the spectral distribution of the radiant power emitted by the external surface, but also the characterization of the viewing conditions. Due to the anatomically and physiologically structure of the human eye (fovea centralis versa the lateral rest of the retina) there already exists a different color impression depending on the size of the surface we are looking at. These different impressions are handled by standard observer definitions with 2º and 10º visual field, which have been introduced by CIE (Commission Internationale de L'Eclairage) in 1931 and 1964.[1]

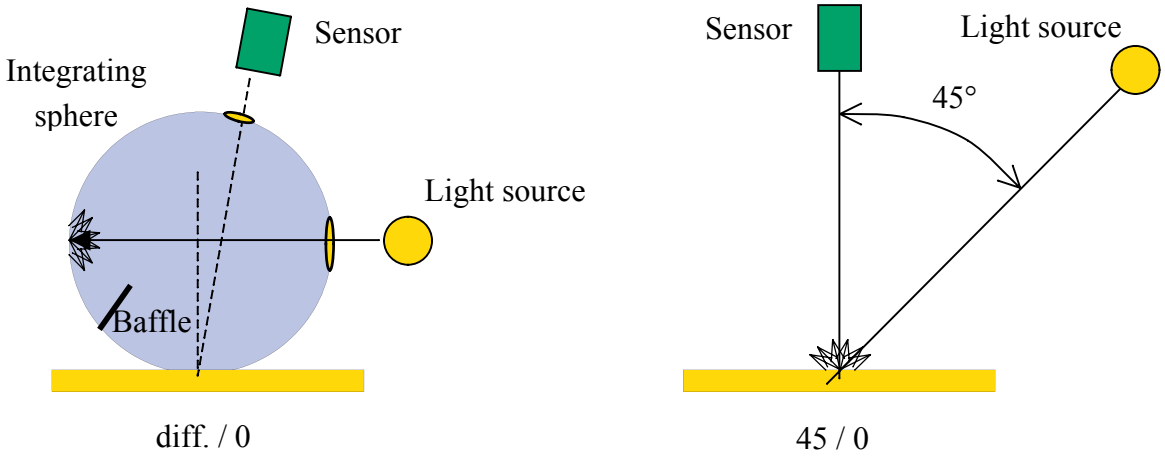

Figure 1: Illumination and viewing geometries

For industrial color measurement there are two different types of illumination and viewing conditions commonly used. One method is using an integrating sphere to produce a perfect diffuse illumination. This method is very precise and not sensitive to direction dependant reflections. Several measurements of the same target will give the same values with high precision. The second method, where the illumination is applied with an angle of incidence of 45° meets the color impression in an everyday surrounding better than the idealized diffuse illumination, which very often is not given in real life. If the target has a structured surface with direction dependant reflection, the second method will give different values for repeated tests with altered surface orientations. Wood is a very anisotropic material with a strong variation of reflectance according to the angle of illumination, the angle of viewing and the orientation of the wood fibers. The purpose of this paper is to study the relations and the relevance for the design of a color inspection system.

According to the human eye, with 3 different types of color sensitive receptors, the representation of color as it appears to a human observer requires a 3 dimensional data space, a so called ***tristimulus space.*** Today this space normally is implemented by cameras, using the typical three color channels RGB. Different systems have been defined for handling color information in a way that makes it easier to handle for human observers. While Funk et. al. [2] have demonstrated, that the choice of a specific color space is not essential for defect detection on wood, a unified color space like the CIE L*,a*,b* color space is better suited for dealing with "color differences" according to the human color impression.

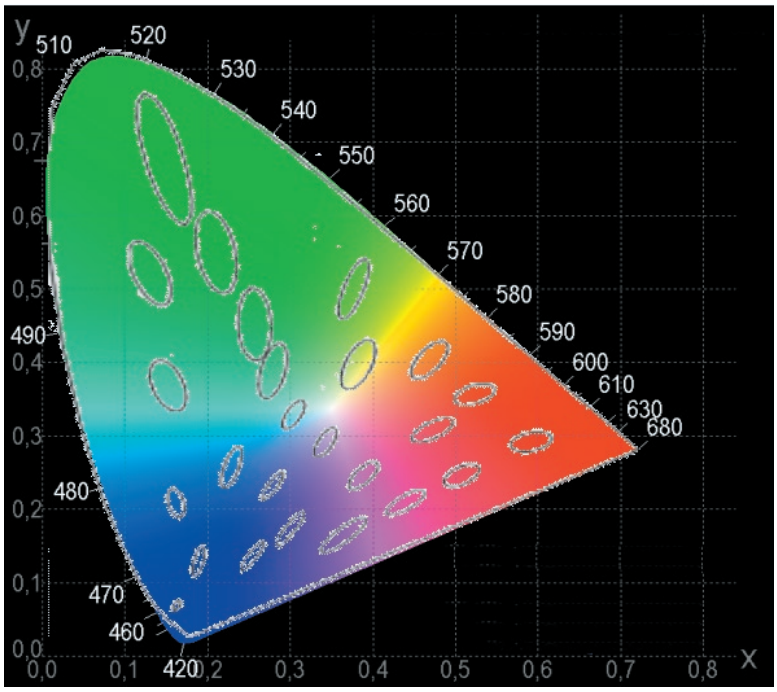

Figure 2: CIE color space and Mc Adams ellipses

The ability of the human eye to differentiate colors with tiny differences in chromaticity is not uniform and was investigated by Mc. Adams[1, pp 666]. Uniform color differences can be shown as ellipses in the xy plot of the CIE 1931 color space.

To improve the precise quantification of perceptual distance between two colors, uniform color spaces CIE L*,u*,v* and CIE L*,a*,b* were introduced [WYS, 166ff]. Both systems are based on the perceived lightness L* and a set of opponent color axes. Today, the CIE L*,a*,b* is the most used model for color matching and was used in our experiments too.

The total color difference ΔE between two color stimuli, each given in terms of L*,a*,b*, is calculated from:

$$(1) \qquad \Delta E^*_{ab} = \sqrt{\left[(\Delta L^*)^2 + (\Delta a^*)^2 + (\Delta b^*)^2\right]}$$

It should be mentioned, that even for the human eye color stimuli of different spectral radiant power distributions can lead to identical tristimulus values and therefore can not be distinguished from each other. They are called metameric stimuli with respect to a given observer. Even though an observer can judge two colors samples illuminated with a specific illuminant identical, they can be distinguished from each other by using another illuminant with a different radiant spectral power distribution.

2. Method and Experiments

2.1 Limitations of typical 8 bit color linescan cameras

To investigate in a first step, which colors in the CIE 1931 color space theoretically can be covered by a color camera we have simulated all possible colors that can be expressed by 3 x 8 bit of a TVI Pricolor linescan camera. The given sensitivity curves of the camera were used for the simulation.

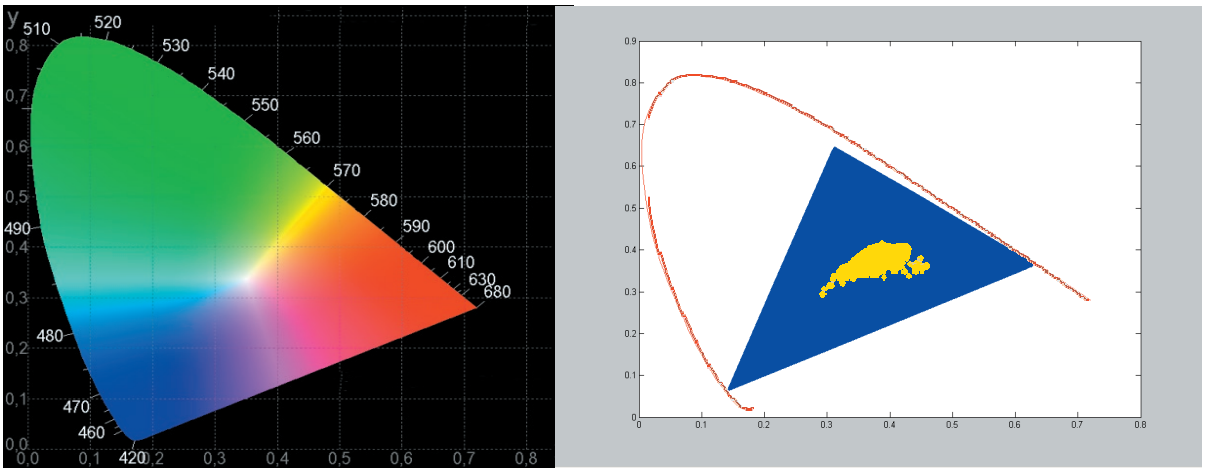

Figure 3 left: CIE 1931 color space,
right: color range covered by 8 bit camera (blue triangle) and typical wood colors (yellow spots)

On the right side of figure 3, the range of colors in the CIE 1931 color space that can be detected with the TVI linescan camera (using 8 bit) is shown as the blue triangle. The yellow spot within this rectangle represents the colors of wood samples for both, softwood and hardwood, coming from 18 different samples of different species of veneer. It is obvious that the complete color space necessary for the description of these typical samples can be clearly covered by the camera.

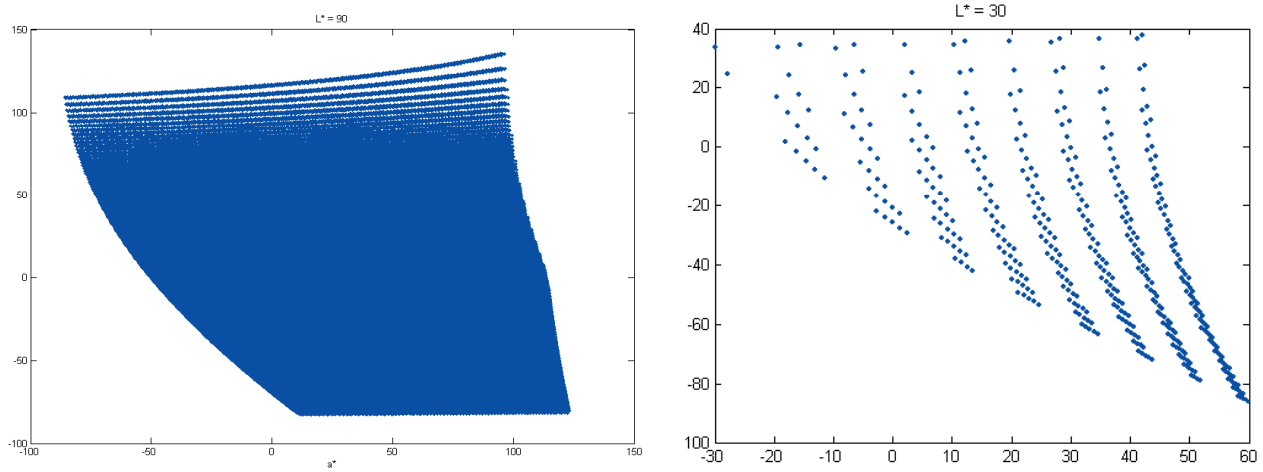

Figure 4: Covered color values by 3 x 8 bit camera, left $L^* = 90$, right $L^* = 30$

Another important question is the theoretical ability of resolving tiny color differences of dark image regions. While the exposure of the camera must be adjusted in a way to handle even the brightest regions of bright samples without clipping, the color resolution naturally decreases for lower RGB values coming from that regions of the target surface with weak reflectance. Therefore, for low L values, the distance in color space of two neighbor colors that can be separated in the RGB signal of the camera is increased.

2.2 Reflectance variations according to the angle of illumination and the orientation of grain

To evaluate the influence of different illumination and viewing arrangements we build up a scanning station with a fixed camera, an imaging spectroscope and a pivoting light source. The axis of rotation is exactly on that line on the surface of the samples on which the camera is looking at through the slit of the imaging spectrograph. An angle encoder gives precise angle information and is used as a trigger for grabbing images every 2° of rotation. The nearest angle to the vertical axis is limited to 8° to avoid occluding the camera view by the fiber optics. The lights can be twisted to a maximum angle of 76° to the vertical axis, resulting in 34 images for each sweep.

One 150W halogen lamp OSRAM EKE in a housing in combination with two fiber optics are used to illuminate the samples.

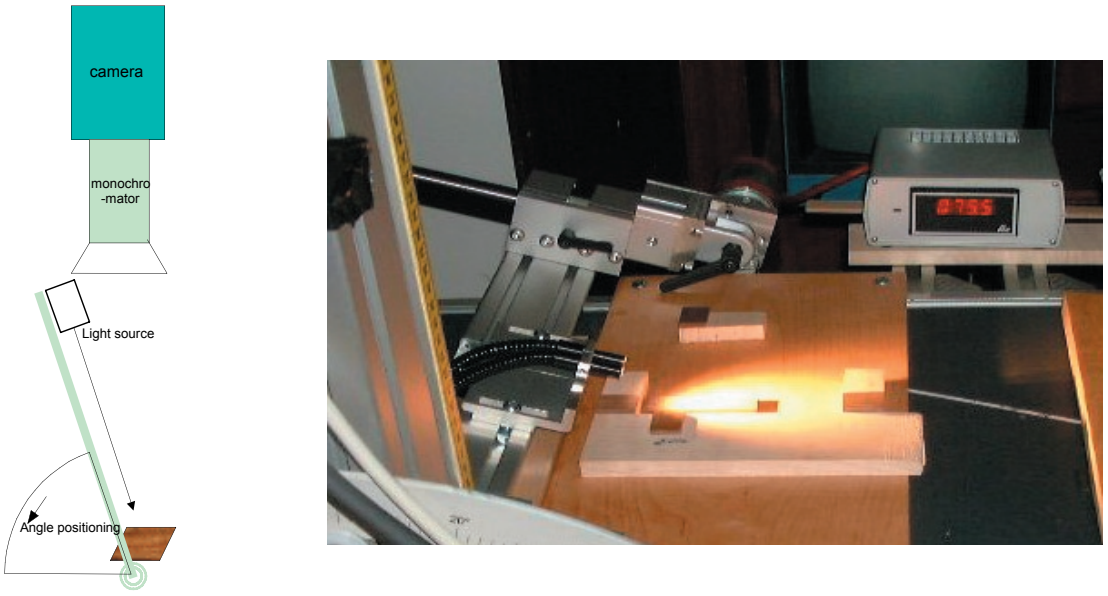

Figure 5: Data acquisition unit for angle dependant reflection measurements

A SPECIM ImSpector imaging spectrograph (400 – 1000 nm, spectral resolution 5 nm) is mounted on a digital 8 Bit camera (JAI CV- M4) with a resolution of 1300 x 1030 Pixels. At each angle an image of a line is grabbed. This 1D line is split into the spectrum inside the spectrometer. This 2D image with geometrical resolved information in the x axis and the spectral information in the y axis is projected onto the CCD chip of the camera.

A spectral calibration of this system is performed using a laser (632,8 nm) and a Hg calibration lamp with well known peaks in the range from 400 – 1000 nm. A second order calibration curve ($\lambda = 0.000083\ x^2 + 0.3917x + 399.1919$) is used to map pixel positions to corresponding wavelengths.

Several given physical limitations are summing up and make it difficult to successfully measure reflectance spectra in the whole visible range of light using CCD silicon cameras:

- low radiant power emission of Hg lamps in the blue range of the spectrum
- low sensitivity of silicon CCD sensors in the blue range of the spectrum
- high emission of Hg lamp in the red range of the spectrum
- high sensitivity of the sensor in the red range of the spectrum

To make it even worse, tilting the light from the perpendicular direction to a real flat illumination increases the necessary dynamic range even more.

Overcoming these limitations would require a camera with a better dynamic range than 8 Bit. Unfortunately those cameras with a high dynamic range using a cooled sensor chip are very expensive and therefore could not be used in the presented work.

The advantage of our experimental set-up is, that we can repeat each scanning of exactly the same line on the sample several times, since there is no movement of the sample or the camera involved. Using a series of exposure times, we are able to considerably increase the dynamic range of our scanning equipment. We are working with exposure times from 4 to 32 ms.

The acquired datasets are combined into one complete data set in such away, that always the best available signal quality is used. Unfortunately the data matching leads to unsatisfactory results with systematic errors. Calibrating the system with a secondary white reflectance normal shows, that the radiometrical sensitivity of the system is not linear.

Correcting this with a linear transfer function for grey values from 0 – 170 and using a second order fitting function from 171 to 255 gives very good results for the complete series of experiments with no observable systematic errors.

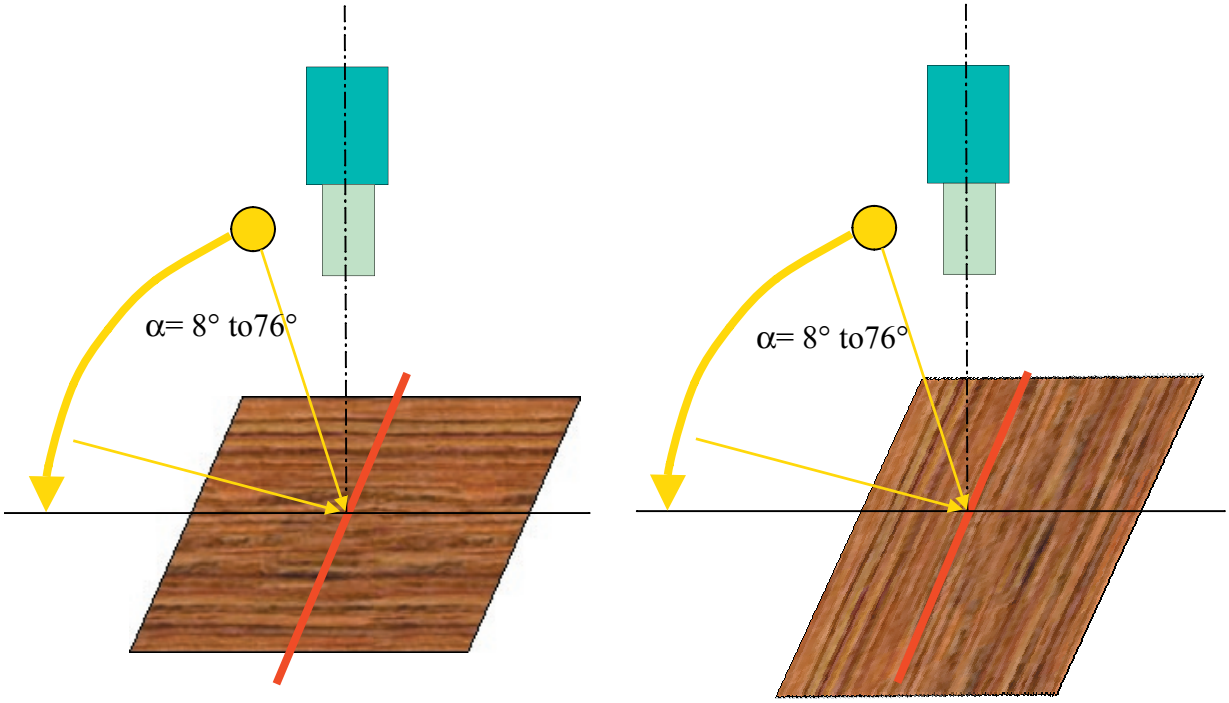

Figure 6: Camera – Illumination – Wood Sample (Grain) Orientation: Left image: Light tilted parallel to grain orientation Right image: Light tilted transverse to grain orientation

Reflectance spectra of 20 samples per wood specie (maple, oak, ash and beech), with two orientations of the grain according to the tilt direction of the illumination, are measured in our study. Each of these samples is scanned at 4 different exposure times, giving a set of 4 x 34 = 136 frames per sample for each orientation.

We started the experiments with a rough surface coming from sawing with an industrial circular saw. Later on we sanded the samples with a very fine graining (1000) in the fiber direction. Sanding makes the observed behavior more clear and removes a lot of "noise" compared to the sawn surface. But the same quality of relations can be observed on both surface treatments.

Calibrating the complete system with a secondary white reflectance standard makes it possible to map the spectra to the CIE L*, a*, b* color space to compare color differences independently from light intensity and accordingly to the color sensitivity of the human eye.

3. Results

Image7 shows typical results of the measurements for an oak sample. For all top row images the sample was scanned with an orientation of the grain parallel to the light tilt direction. In image *a*, the top most line is one fixed line on the sample, illuminated under an angle of $\alpha = 8°$ with respect to the vertical axis. The next line down represents the same line on the surface of the wood, illuminated at an incidence angle of $\alpha = 10°$. The decrease of L* is compensated to make it easier to view only color changes (a*, b*), not the known decrease of L*. The angle is increasing every line up to 76° in steps of 2°. Image *b* is the plot of the L*, a*, and b* components, plotted for all pixel positions of the scanned line. Image c is a plot of the color distance for each pixel to the color value at an illumination angle of 8° as a function of illumination angle. The color distance is computed according to formula (2)

$$\Delta_{ab} = \sqrt{(a^*_{8°} - a^*_{\alpha})^2 + (b^*_{8°} - b^*_{\alpha})^2} \qquad (2)$$

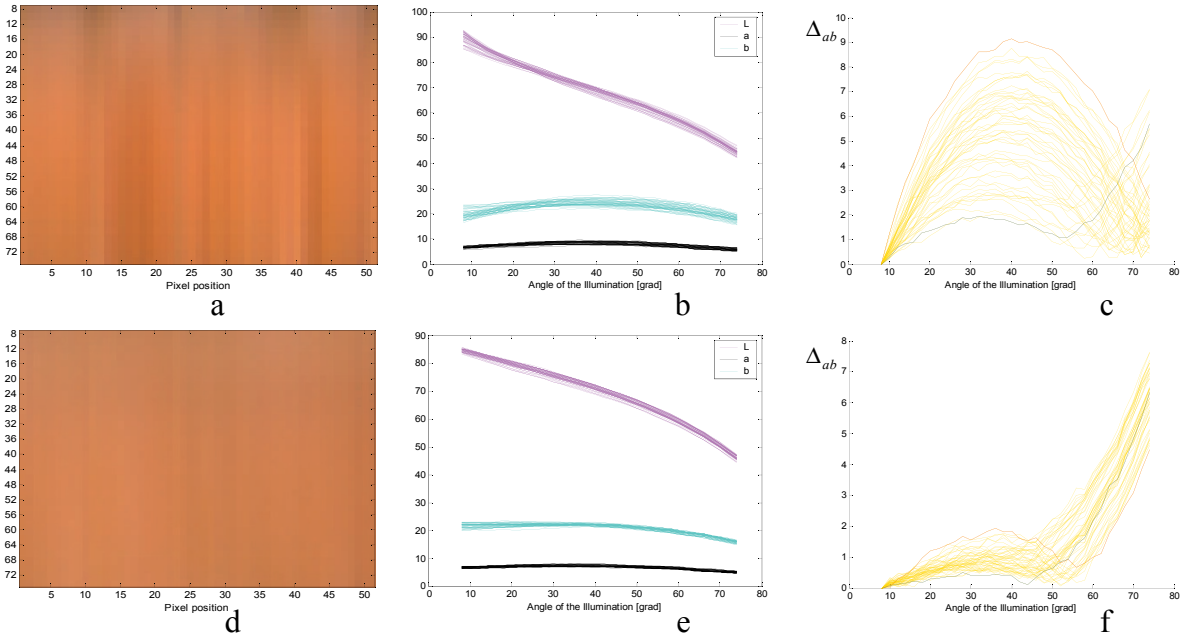

Figure 7: top row, images a, b, c – grain parallel to light tilt direction
bottom row, images d, e, f – grain transverse to light tilt direction

Images 7 *d,e,f,* are the corresponding images, with the orientation of the grain transverse to the light tilt direction.

The evaluations for this paper are concentrated on color shift, not on the decrease of illumination as it can be seen in images 7 *b+e*. More interesting are the curves in images 7 *c+f* , which demonstrates a different behavior of color changes according to the grain orientation. The yellow curves are the Δ_{ab} values for all different pixels in the line as a function of α, and the red and blue curves are the plots of two pixels, which have a minimum or a maximum difference Δ_{ab} at a certain angle α respectively.

When tilting the light parallel to the grain orientation, an increase of the color deviation up to an angle of 30 ° to 45° is clearly visible. For angles between 45° and 70° Δ_{ab} decreases, before it is increasing again very strongly for flat illumination. When tilting the light transverse to the grain orientation, the color change is low ($\Delta_{ab} \leq 2$) up to an angle of 45° to 55°, before increasing strongly above that angle.

In figure 8, the average color distances of all pixels in the scanning line of 5 different oak samples are plotted for both grain directions. The average color deviation does not have that strong difference for the two orientations of grain compared to single pixels, although the trends we previously found for single pixels is still remaining.

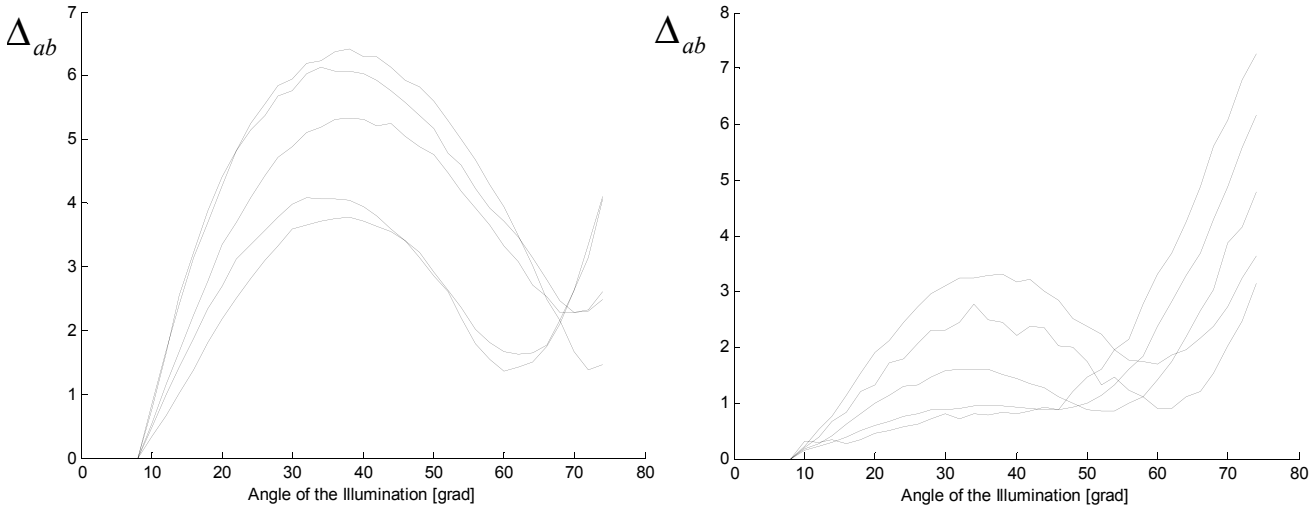

Figure 8: Average of Δ_{ab} over all pixels of 5 different oak samples, left image: grain parallel to light tilt direction, right: grain transverse to light tilt direction

In figures 9, 10 and 11 the color deviation for respectively an ash, a beech and a maple sample is plotted.

For ash, the direction dependency is very clear too. When tilting the light transverse to the grain, a very low change in color can be observed up to 40°. When illuminating parallel to the grain, the deviation is comparable to the one of oak.

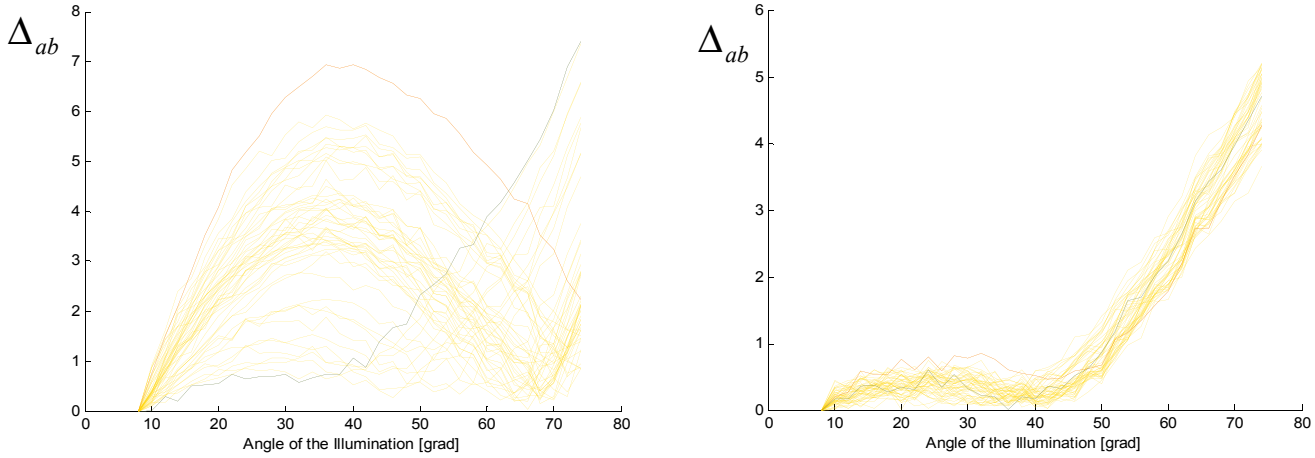

Figure 9: Δ_{ab} of ash sample
left image: grain parallel to light tilt direction, right: grain transverse to light tilt direction

Beech samples show a comparable behavior to ash.

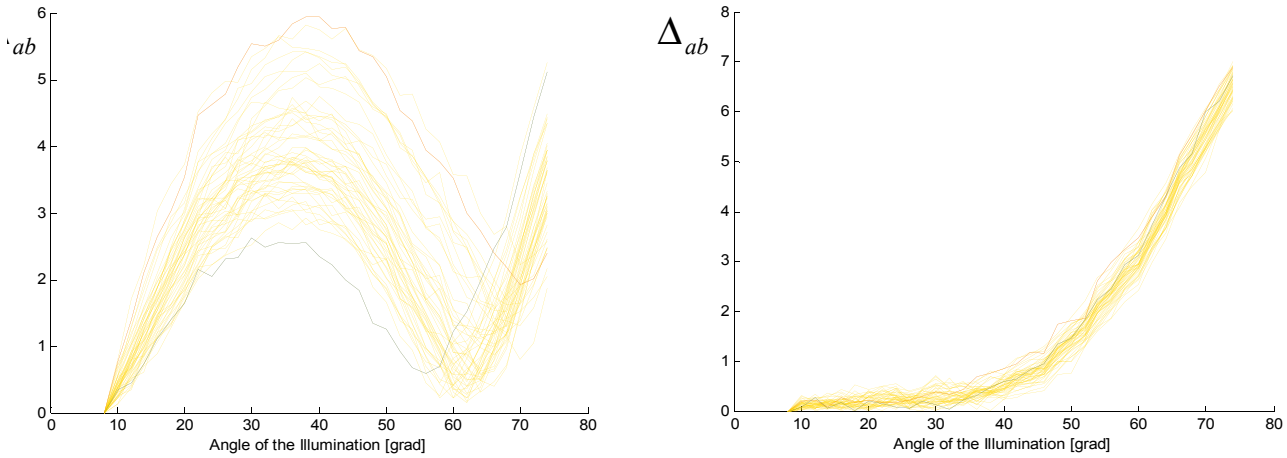

Figure 10: Δ_{ab} of beech sample
left image: grain parallel to light tilt direction, right: grain transverse to light tilt direction

Maple samples have a comparable low color change when tilting the light parallel to the grain up to an angle of 45°. Tilting the light transverse to the grain leads to a considerable strong increase of Δ_{ab} even for small angles α.

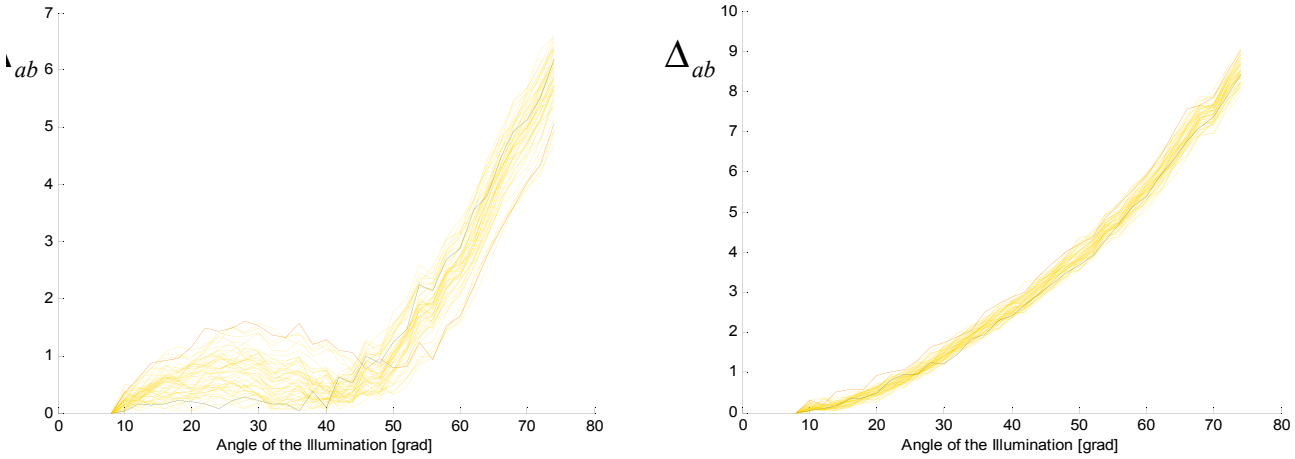

Figure 11: Δ_{ab} of maple sample
left image: grain parallel to light tilt direction, right: grain transverse to light tilt direction

Conclusions

The color difference expressed as $\Delta_{ab} = \sqrt{(a^*_{8°} - a^*_{\alpha})^2 + (b^*_{8°} - b^*_{\alpha})^2}$ between a reference illumination position (8°) and the test illumination positions (10°-76°) is not only a function of the incidence angle, but is also strongly dependant on the orientation of the grain relative to the light. There is also a different behavior for different wood species.

More experiments should be made to investigate the direction dependency of reflections of specific wood discoloration caused by fungi attacks. These defects often have the effect of destroying the cell walls and therefore will change the reflectance behavior of the samples in addition to the observed phenomenon.

Traditional Kubelka-Munk [1, pp 221] theory cannot be applied directly to describe this behavior, because wood is a material with a cellular structure and therefore different directional characteristics compared to ideal scattering media.

A modified "Directional characteristics model", proposed by Tsuchikawa et al. [3] as a theoretical basis can better explain the observed relation between the direction of the incoming light and the direction of wood grain. This model suggests, that the reflected light is composed from diffusely reflected components from the inner cell and also from the semi-specular multiple reflected light from each cell wall surface. The semi-specular reflection is strongly related to the wavelength and the direction of the incoming light.

Literature

[1] Wyszecki, Stiles, "Color Science", *Wiley Classics Library Edition Published 2000*

[2] J. Funk, D. Butler, C. Brunner, J. Forrer, Y. Zhong, A performance analysis of image segmentation algorithms as applied to wood surface feature detection, in *Proceedings of the 4th International Conference on Image Processing and Scanning on Wood*, Mountain Lake Resort, Virginia, USA, August 2000, pp 129 – 142

[3] S. Tsuchikawa, Non-traditional applications of near infrared spectroscopy based on the optical characteristic models for a bilogical material having cellular structure, *Near Infrared Spectrosc*., 6 ,41-46, (1998)

[4] S. Tsuchikawa, M. Torii, S. Tsutsumi, "Directional characteristics of near infrared light in the process of radiation and transmission from wood", *Near Infrared Spectrosc*., 6, 47-53, (1998)

Alfred Rinnhofer, Wanda Benesova, Gerhard Jakob, Roman Benes